SENSING OF THE ATMOSPHERE WITH THE HIRS/2 SATELLITE IR-RADIOMETER

S.V. Afonin, A.D. Bykov, Yu.V. Gridnev, V.V. Zuev, M.Yu. Kataev, V.S. Komarov, A.A. Mitsel', O.V. Naumenko, K.M. Firsov, T.Yu. Chesnokova, and A.A. Chursin

Institute of Atmospheric Optics,
Siberian Branch of the Russian Academy of Sciences, Tomsk
Received July 2, 1998

Feasibility of sensing of the vertical profiles of the air temperature and total content of H_2O, O_3, *and* N_2O *in the atmospheric column above the territories of the Tomsk and Novosibirsk regions from measurements with HIRS/2 is analyzed. The regression methods of reconstructing the total* H_2O *content are described. The influence of the uncertainty in the initial spectroscopic information on the error in reconstructing temperature profiles is considered. The most important problems are formulated whose solution will provide the development of reliable technique for reconstructing the meteorological parameters of the atmosphere.*

INTRODUCTION

Satellite remote sensing instruments find expanding application for spaceborne geophysical research. At present they are widely used for solving problems in various branches of man's activity including agriculture, meteorology, ecological monitoring of the environment, and military applications.

In 1997 the IAO of the SB RAS established a station to receive the data from NOAA series satellites (NOAA–12 and NOAA–14). Each satellite has a circumpolar orbit synchronous with the Sun with a revolution period of about 102 min (see Ref. 1). Two orbiting satellites provide, on average, 4 observations a day for most sites on the Earth's surface. Four instruments are placed onboard the satellites: HIRS/2, AVHRR, MSU, and SSU. In the present paper we study the capabilities of HIRS/2 for determining the total content of gaseous constituents and the vertical temperature profile in the atmosphere.

SPECIFICATIONS OF HIRS/2

The HIRS/2 instrument is a modification of HIRS/1 placed on board NIMBUS–6. It was developed by the Aerospace Optics Department of the International Telegraphic–Telephonic Corporation (ITT, Fort Wayne, Indiana). The HIRS/2 radiometer records radiation in 19 IR channels and one visible channel. The characteristics of the channels and their designation are given in Tables I and II. Specifications of the radiometer are given in Table III. All these data were borrowed from Ref. 2 and Internet sites.

TABLE I. Spectral characteristics of HIRS/2 (NOAA-14).

Serial number of channel	Central frequency ν, cm^{-1}	Central wavelength, μm
1	669	14.95
2	679	14.72
3	690	14.5
4	703	14.21
5	703	14.21
5	714	13.99
6	732	13.65
7	750	13.34
8	899	11.1
9	1028	9.72
10	796	12.56
11	1361	7.35
12	1481	6.75
13	2191	4.56
14	2207	4.53
15	2236	4.47
16	2268	4.41
17	2420	4.13
18	2512	3.98
19	2648	3.77
20	14367	0.7

0235-6880/98/10 914-09 $02.00

TABLE II. Channels of the HIRS/2 radiometer and their designation according to Ref. 2.

Serial number of channel	Wavelength, μm	Designation
1–7	14.95–13.35	Temperature profiles
5–7		Cloud altitude and amount
8	11.11	
9	9.71	Total ozone content
10–12	8.16–6.72	Water vapor profiles, detection of thin cirrus clouds
13–17	4.57–4.24	Temperature profiles
18–20	4.00–0.69	Clouds, surface temperature under conditions of broken cloudiness

TABLE III. Specifications of HIRS/2 according to Ref. 2.

Parameter	Value
Transverse scan	± 49.5° (± 1125 km)
Scanning time	6.4 s per a line
Number of steps	56
Optical field-of-view angle	1.25°
Angular step	1.8°
Temporal step	100 ms
Resolution on the Earth's surface (in the nadir)	17.4 km in diameter
Spatial resolution on the Earth's surface at the end of scan	58.5 km in the transverse direction of the scan × 29 km along the scan
Data sampling rate	2880 bits per 1 s

DATA CALIBRATION

General calibration technique of satellite radiometers was considered in Ref. 3. The calibration procedure was described in Ref. 2. Calibration is carried out in flight every 256 s (40 scanning lines) by sighting on two targets placed on board the satellite (a hot target with T = 290 K and a cold target with T = 260–270 K) and onto the outer space (T = 0.3 K). The temperature of targets is measured with built-in thermistors. The temperature of the cold target cannot be measured with satisfactory accuracy due to large temperature gradients caused by the influence of the Sun; therefore, in practice only the hot target and the outer space (T = 0.3 K) are used for calibration.

In practice, the calibration is performed as follows: first, the temperature T_{ht} of the hot target is measured with four thermistors (each measurement is averaged over 5 readings of individual thermistor). The measured values are stored as data item No. 58 of the HIRS/2 data set (a total of 40 lines, as indicated above, is used for calibration, that is, 40×5 = 200 readings of each thermistor). The average reading of the termistor is calculated from the formula

$$X_k = \frac{1}{200} \sum_{i=1}^{40} \sum_{j=1}^{5} X_{ij}, \quad k = 1, 2, 3, 4.$$

The temperature T_k measured with each thermistor is then calculated based on the simple formula

$$T_k = a_0 + a_1 X_k + a_2 X_k^2 + a_3 X_k^3 + a_3 X_k^4,$$

where X_k is the value averaged over 200 readings of the kth thermistor, and a_j are the scale factors tabulated in Ref. 2 and on Internet sites.

The temperature of the hot target is calculated as an average of readings of all thermistors

$$T_{\text{ht}} = \frac{1}{5} \sum_{k=1}^{5} T_k.$$

The radiance N recorded in the given channel from the target can be calculated from the known value of T_{ht} based on the formulas and tables from Ref. 2. We note that there are two methods for calculating this radiance:

1. An efficient temperature T_{ef} calculated from the formula

$$T_{\text{ef}} = b + c\, T_{\text{ht}},$$

is used instead of T_{ht}, where the coefficients b and c are tabulated in Ref. 2 and on Internet sites for the examined satellites.

Then the radiance is calculated from the Planck formula

$$N_{\text{ht}} = c_1 \nu_i^3 / [\exp(c_2 \nu_i / T_{\text{ef}}) - 1],$$

where i = 1, 19 are the serial numbers of channels, and c_1 and c_2 are the standard coefficients in the Planck formula, namely, $c_1 = 1.1910659 \cdot 10^{-5}$ mW/(m^2·sr·cm^{-1}) and c_2 = 1.438833 cm·K.

2. The radiance can be calculated in terms of the instrumental functions of channels

$$N(T) = \frac{\int_{\nu_1}^{\nu_2} B(\nu, T)\, \Phi(\nu)\, d\nu}{\int_{\nu_1}^{\nu_2} \Phi(\nu)\, d\nu},$$

where $B(\nu, T)$ is the Planck function and $\Phi(\nu)$ is the spectral response function of the channel tabulated in Ref. 2 and on Internet sites.

The final formula to convert the readings of the instrument X_E to the radiance N_E coming from the Earth has the form

$$N_E = M\,X_E + I,$$

where M is the so-called steepness of the channel, and I is its displacement. A procedure for the determination of these parameters was described in detail in Ref. 2. They can be calculated from the formulas

$$M = \frac{N_{\rm sp} - N_{\rm ht}}{X_{\rm sp} - X_{\rm ht}}\,;\; I = N_{\rm sp} - MX_{\rm sp},$$

where $N_{\rm sp}$ and $N_{\rm ht}$ are the radiances from the outer space and the hot target, respectively; $X_{\rm sp}$ and $X_{\rm ht}$ are the corresponding average readings of the instruments calculated from the formulas

$$X_{\rm sp} = \frac{1}{48}\sum_{j=1}^{48} X_{\rm sp}(j);\; X_{\rm ht} = \frac{1}{56}\sum_{j=1}^{56} X_{\rm ht}(j).$$

SENSITIVITY OF THE HIRS/2 CHANNELS TO VARIATIONS IN THE ATMOSPHERIC PARAMETERS

Variability of the upwelling radiation measured with the HIRS/12 and HIRS/14 radiometers is caused primarily by two factors, namely, by variations of the vertical temperature profiles and underlying surface temperature and by the presence or absence of cloudiness of different types. The variability of the vertical profiles of concentrations of atmospheric gases has much less of an effect on the variations of radiance.

Tables IV and V illustrate the sensitivity of the HIRS/14 channels to the variability of temperature and total content of atmospheric gases for two meteorological models. The upwelling radiance in the atmosphere received with the radiometer was calculated considering the instrumental function of each channel. Then it was converted to the radiative temperature. The second columns give the central frequency of the transmission band of the light filter. The radiative temperature is given in the third columns. The last columns illustrate the change in the radiative temperature when the entire vertical temperature profile is changed by 2 K. In calculations, the emissivity of the underlying surface was taken to be unity, that is, the reflected radiation was absent. The temperature of the underlying surface was equal to that of the atmospheric layer adjacent to it.

The sensitivity of the radiometer to the variations of the CO_2 content is illustrated by Tables IV and V for generality of presentation. In atmospheric sensing with HIRS, the channels, in which the absorption is due to carbon dioxide, are used to retrieve the temperature. Because this radiometer has only limited number of channels, simultaneous retrieval of the vertical temperature profiles and CO_2 content is impossible; therefore, the CO_2 concentration is assumed to be known. An analysis of these tables indicates that the sensitivity of the radiometer to variations of CO and CH_4 concentrations is also low. As a consequence, the content of these gases cannot be reconstructed. It also can be seen that, to retrieve the concentrations of H_2O, O_3, and N_2O, the uncertainty in the atmospheric state caused by the uncertainty of the underlying surface temperature, vertical temperature profiles, aerosol extinction, and cloudiness should be at least within 1–2°.

Particular attention should be given to the influence of the dry land underlying surface. Its emissivity may vary in wide limits and its spectral dependence, unlike the water surface, cannot be predicted. Our estimates demonstrate that the error in determining the underlying surface temperature may be as great as, 5 K. Table VI presents the results of modeling, when the underlying surface temperature differed from the adjacent air temperature by 5 K. Comparing Tables IV and V with Table VI, we note that the error in determining the total ozone content caused by possible errors in determining the underlying surface temperature may be as great as 30% and more. In case of sensing of the N_2O content, channels 13 and 14 are also very sensitive to the uncertainty in assignment of the underlying surface temperature. The influence of the underlying surface temperature reduces to minimum only for channel 15.

The HIRS radiometer is sensitive to variations of water vapor content in channels 7, 8, 10–12 for summer months and in channels 11–12 for winter months. It follows from Table V that in channels 7, 8, and 10 the radiative temperature in winter is very sensitive to the uncertainty in assignment of the underlying surface temperature, whereas in summer this is true only for channel 10.

From the foregoing it can be seen that the procedure for H_2O reconstruction should be based on the data of channels 7, 11, and 12, whereas the corresponding procedure for N_2O reconstruction should be based on data of channels 14 and 15. We have only channel 9 to reconstruct the O_3 concentration, which may cause large errors. Together with the influence of the underlying surface temperature, additional error may be introduced, because the altitude of the ozone layer is unknown.

TABLE IV. Sensitivity of the HIRS/14 channels to the variability of the temperature and vertical profiles of concentrations of atmospheric gases calculated for the summer meteorological model at mid-latitudes.

Serial number of channel	ν, cm^{-1}	T_r	Change in the radiative temperature attendant to a 30% change of the total content of the atmospheric gas						$T_{\pm 2}$
			H_2O	CO_2	O_3	N_2O	CO	CH_4	
1	668.90	238.73	0.00	1.27	0.04	0.00	0.00	0.00	1.96
2	679.36	228.03	0.00	1.05	0.10	0.00	0.00	0.00	1.95
3	689.63	226.59	0.00	0.44	0.09	0.00	0.00	0.00	1.98
4	703.56	235.25	0.08	1.99	0.04	0.00	0.00	0.00	1.76
5	714.50	246.73	0.22	2.71	0.18	0.00	0.00	0.00	1.67
6	732.28	261.24	0.55	2.99	0.28	0.00	0.00	0.00	1.73
7	749.64	172.71	1.03	1.87	0.23	0.00	0.00	0.00	2.06
8	898.67	291.97	0.99	0.00	0.00	0.00	0.00	0.00	2.06
9	1028.31	268.88	0.43	0.04	3.22	0.00	0.00	0.00	2.01
10	796.04	287.04	1.49	0.26	0.04	0.00	0.00	0.00	1.99
11	1360.95	258.97	1.97	0.00	0.00	0.00	0.00	0.43	1.92
12	1481.00	242.48	1.79	0.00	0.00	0.00	0.00	0.01	2.01
13	2191.32	278.54	0.26	0.01	0.00	2.13	0.18	0.00	1.85
14	2207.36	269.30	0.21	0.08	0.00	3.40	0.08	0.00	1.94
15	2236.39	257.37	0.08	1.26	0.00	2.82	0.00	0.00	1.79
16	2268.12	235.75	0.01	2.06	0.00	0.02	0.00	0.00	1.92
17	2420.24	287.77	0.08	1.70	0.00	0.00	0.00	0.00	2.01
18	2512.21	293.79	0.08	0.00	0.00	0.04	0.00	0.00	2.01
19	2647.91	292.80	0.32	0.00	0.00	0.01	0.00	0.00	2.01

TABLE V. Sensitivity of the HIRS/14 channels to the variability of the temperature and vertical profiles of concentrations of atmospheric gases calculated for the winter meteorological model at arctic latitudes.

Serial number of channel	ν, cm^{-1}	T_r	Change in the radiative temperature attendant to a 30% change of the total content of the atmospheric gas						$T_{\pm 2}$
			H_2O	CO_2	O_3	N_2O	CO	CH_4	
1	668.90	222.75	0.00	0.72	0.01	0.00	0.00	0.00	2.00
2	679.36	217.30	0.00	0.14	0.01	0.00	0.00	0.00	1.99
3	689.63	217.26	0.00	0.03	0.01	0.00	0.00	0.00	2.00
4	703.56	223.71	0.03	1.41	0.08	0.00	0.00	0.00	1.783
5	714.50	231.48	0.03	1.91	0.22	0.00	0.00	0.00	1.76
6	732.28	241.15	0.05	1.87	0.26	0.00	0.00	0.00	1.80
7	749.64	248.92	0.07	1.06	0.20	0.00	0.00	0.00	1.81
8	898.67	257.16	0.02	0.00	0.00	0.00	0.00	0.00	2.00
9	1028.31	238.89	0.00	0.01	2.27	0.00	0.00	0.00	2.01
10	796.04	256.32	0.09	0.11	0.03	0.00	0.00	0.00	1.97
11	1360.95	245.85	1.07	0.00	0.00	0.00	0.00	0.43	1.93
12	1481.00	233.75	1.59	0.00	0.00	0.00	0.00	0.01	2.01
13	2191.32	249.14	0.01	0.00	0.00	1.25	0.11	0.00	1.91
14	2207.36	242.80	0.01	0.03	0.00	2.20	0.05	0.00	1.98
15	2236.39	235.69	0.01	0.73	0.00	1.94	0.00	0.00	1.88
16	2268.12	221.74	0.00	1.05	0.00	0.01	0.00	0.00	1.98
17	2420.24	254.12	0.00	0.88	0.00	0.00	0.00	0.00	2.01
18	2512.21	257.12	0.00	0.00	0.00	0.02	0.00	0.00	2.00
19	2647.91	257.09	0.03	0.00	0.00	0.01	0.00	0.00	2.00

TABLE VI. Sensitivity of the HIRS/14 channels to variability of the underlying surface temperature which was changed by ±5°.

Serial number of channel	ν, cm^{-1}	Summer mid-latitudes		Winter at arctic latitudes	
		T_r	ΔT	T_r	ΔT
1	668.90	238.73	0.00	222.75	0.00
2	679.36	228.03	0.00	217.30	0.00
3	689.63	226.59	0.00	217.26	0.00
4	703.56	235.25	0.00	223.71	0.04
5	714.50	246.73	0.07	231.48	0.33
6	732.28	261.24	0.33	241.15	1.15
7	749.64	272.71	0.77	248.92	2.52
8	898.67	291.97	3.48	257.16	4.90
9	1028.31	268.88	2.44	238.89	2.84
10	796.04	287.04	2.03	256.32	4.39
11	1360.95	258.97	0.00	245.85	0.48
12	1481.00	242.48	0.00	233.75	0.00
13	2191.32	278.54	2.43	249.14	2.79
14	2207.36	269.30	1.47	242.80	1.54
15	2236.39	257.37	0.68	235.69	0.73
16	2268.12	235.75	0.01	221.74	0.01
17	2420.24	287.77	3.53	254.12	3.42
18	2512.21	293.79	4.82	257.12	4.95
19	2647.91	292.80	4.39	257.09	4.85

RETRIEVAL OF THE TOTAL CONTENT OF O_3, H_2O, AND N_2O

The problem of reconstructing the total content of gases can be solved in two ways. By the first procedure, we first reconstruct the temperature profile for the channels with predominant absorption of radiation by CO_2. Then the temperature of the underlying surface is reconstructed from measurements in transparent channels, and in the last stage the total gas content or its concentration at the given altitudes is retrieved. This approach was implemented in the procedure for determining the total ozone content described in Ref. 4. To this end, the brightness temperatures in channels 1, 3, 8, 10, 18, and 19 of the HIRS radiometer and in channel 4 (57.94 GHz) of the MSU apparatus were used.

This procedure is based on an adequate two-layer physical model of radiative transfer; the thermal characteristics of these layers are determined from measurements in other channels of HIRS and MSU, whereas the variations in the ozone content are retrieved from a signal measured in the 9.7-μm channel.

An algorithm for reconstructing the ozone content can be physically justified as follows: in the present paper we investigate the influence of deviations of the ozone content from its standard profile described in Ref. 5 on the transmission of radiation in the 9.7-μm channel. The ozone content in different layers and classification of these layers for the two-layer model are given in Table VII.

TABLE VII. Ozone layers for the standard profile and the two-layer model.

Layer	Altitude range, km	Pressure, hPa	Standard ozone content, Dobson units	Name of the layer in the two-layer model
Upper	38–54	0–4	16	Upper
Middle	23–38	4–31	143	Upper
Lower	4–23	31–600	177	Lower
Surface	0–4	600–1000	9	Not use

It is obvious that the radiation emitted by the surface around 9.7 μm will be absorbed and re-emitted by ozone; moreover, a significant portion of it (40%) will be absorbed in the layer between 4 and 23 km. Thus, the warm emission of the surface will be replaced by the cold emission of the stratosphere and hence variations in the ozone concentration will affect the measurements of the brightness temperature with HIRS in the 9.7-μm channel. Neuendorffer[4] pointed out that the increase of the ozone content in the lower stratosphere (or in the upper troposphere) by 15 Dobson units leads to the decrease of the brightness temperature in the 9.7-μm channel by 1°.

The second procedure for reconstructing the concentration of one or another gas is based on a correlation between the radiative temperatures in individual channels and gas concentrations. Advantages of this approach are on the one hand, that it obviates the necessity for solving the inverse problem, and on the other hand, that it can be used to evaluate the influence of the uncertainty caused by variability of the atmosphere on the error in determining the gas concentration. As an example, we refer to the regression procedure for reconstructing the H_2O content.[6]

In the first approximation, a model of atmospheric water vapor content can be described by the multiple linear regression equation. It specifies the dependence of the water vapor content in the atmosphere (variable y) on the radiative temperatures (independent variables x_k) measured in different channels of the satellite radiometer for N situations

$$y_i = b_0 + b_1 x_{1i} + \ldots + b_p x_{pi} + e,$$

where $i = 1, \ldots, N$ is the number of observations, $N = 117$ for the summer atmospheric model of Novosibirsk; and p is the number of channels.

To develop the procedure, we took channels 4–16 of the radiometer. The regression coefficients b_0 and b_1 (for channel 4), b_2 (for channel 5) and so on for the examined channels are calculated from the condition of minimization of a sum of square deviations

$$S = \sum_{i=1}^{N} (y_i - b_0 - b_1 x_{1i} - \ldots - b_p x_{pi})^2,$$

Then the statistical significance of the hypothesis that $b_k = 0$, that is, that we can neglect the contribution of the variable x_k to the total content of water vapor to improve the prediction of the variable y, is tested. The level of significance $\alpha = 0.05$ was chosen in hypothesis testing. If the calculated value of p is greater than α, the hypothesis that $b_k = 0$ will be true, and the channel will be excluded from consideration. Channels 4, 11, and 14 for which p was less than α were left by the method of successive selection. The corresponding regression coefficients are given in Table VIII. The curves in Fig. 1 show the error in reconstructing the total water vapor content from measurements in three channels. The use of channels 4, 11, and 14 yields the best results for winter. The error in reconstruction from measurements in a single channel nearly doubled. Analogous results were obtained when we reconstructed the water vapor content from measurements performed simultaneously in all channels 4–16.

The procedure for determining the total H_2O content considered above implies that the underlying surface temperature (UST) is known. Therefore, its further refinement is connected with the determination of the UST. To this end, additional measurements in channels of AVRR and MSU are required.

The reconstruction of the N_2O concentration also presents considerable difficulties, because of the fact that this gas absorbs in channels 13–15 in which the underlying surface makes noticeable contribution to the upwelling radiance (see Table VI). Therefore, measurements in the AVHRR channels should be used in addition to those in the HIRS channels to retrieve the total content of N_2O.

TABLE VIII. Linear regression coefficients for the winter atmospheric model of Novosibirsk.

Serial number of channel	Regression coefficients	Root-mean square error in calculations of the coefficients b_k
	$b_0 = 0.19759$	0.83788
4	$b_1 = -0.02355$	0.00488
11	$b_2 = -0.05669$	0.00353
14	$b_3 = 0.08018$	0.0033

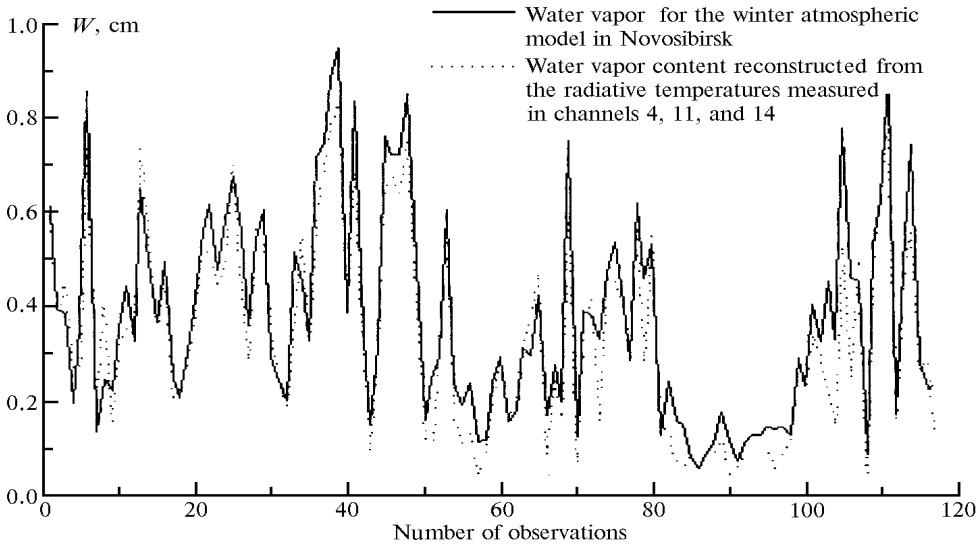

FIG. 1. Total content of water vapor in the atmospheric column in winter reconstructed from the model radiative temperatures in three channels by the multiple linear regression method.

DETERMINATION OF VERTICAL PROFILES OF THE ATMOSPHERIC TEMPERATURE

The basic relation between the measurable parameter (the upwelling radiance, UR) and the vertical temperature distribution in the atmosphere is described by the radiative transfer equation in its integral form. The UR on the upper boundary of the atmosphere (considering that the radiation propagates from the upper atmospheric boundary to the satellite

without attenuation and transformation) can be represented in the following form:

$$I_\nu(\mu) = \delta_\nu B_\nu(T(h_0))\, P(h_0, H_0, \mu) + \int_{h_0}^{H_0} B_\nu(T(z)) \frac{dP_\nu(z, H_0, \mu)}{dz} dz + I_\nu^0(\delta_\nu, \mu), \quad (1)$$

where ν is the central frequency of the channel, δ_ν is the underlying surface emissivity (for a blackbody $\delta_\nu = 1$) at the given viewing angle, $\mu = 1/\cos\varphi$, φ is the angle counted off from the nadir, P is the transmission of the atmospheric layer $(z - H_0)$ in the direction φ, B_ν is the Planck function at the given frequency of the channel and temperature T, h_0 is the altitude of the lower boundary and H_0 is the altitude of the upper boundary of the atmosphere (we take $H_0 = 100$ km in the solution of our problem), and I^0 is the radiance reflected from the Earth's surface.

Channels 1–7 are most informative for reconstruction of the atmospheric temperature,[7] because they comprise the 15-μm absorption band of CO_2. In this case, it is assumed that the CO_2 content is known or it specified by a model. To refine the CO_2 content, channel 16 can be used together with the above-indicated channels (see Table I). In addition, the UST should be known.

We note that whereas the problem of remote sensing of the oceanic surface temperature from measurements of outgoing IR-radiation in the 10.5–12.5-μm window has been developed to real-time engineering level, the problem of remote sensing of the dry-land temperature has not yet been solved adequately, because of the necessity of considering additional factors,[13] namely, deviation of the underlying surface from a blackbody emitter, that is, variations of its emissivity as a function of soil type and state, and significant spatiotemporal variability of the temperature field.

The method of the so-called splitted atmospheric transparency windows[9] based on the use of a linear combination of measurements in channels 10.5–11.5 and 11.5–12.5 μm to estimate the radiation attenuation in the atmosphere (the main factor that interferes with temperature measurements) is well known in the literature. However, this method is ineffective for measurements above the dry land, because the emissivity of the underlying surface in place of sensing must be specified in it with high accuracy (better than 0.01).

An original method for estimating the dry-land temperature with an accuracy of 1–2° from satellite measurements in the wavelength range 10.5–12.5 μm was suggested in Ref. 13. This method is based on the idea of so-called temperature-invariant spectral indices[14] (TISI) – special nonlinear combinations of measurements in two or three channels independent of the dry-land surface temperature – and measurements in channels 4 and 5 of AVHRR and channel 8 of HIRS/2 coincident in space and time. The average vertical profiles of the temperature and water vapor content are also required to implement this method.

In our opinion, the problem of determining the UST for the dry land has yet to be solved and calls for further investigations. For this reason, in the present paper we determine the vertical profile of the atmospheric temperature under assumption that the UST and the temperature of the air layer adjacent to it coincide.

One more problem in temperature sensing is the necessity of solving the Fredholm equation of the first kind. It is well known that the solution of this equation is unstable. At present various methods for solving the problem of temperature sensing are developed with the use of information about the examined temperature profile.[7,8,15] An approach based on the Green's function method for solving the integro-differential equation that appears when the Tikhonov regularization algorithm is applied with a stabilizer of the first order[16] was suggested in Ref. 7.

Examples of solving the model problem with 0.5 and 3% noise level in the right-hand side of the equation is shown in Figs. 2 and 3. The calculations were done for the summer atmospheric model at mid-latitudes. It can be seen from the figures how unstable is the real model problem to the measurements errors. An error of 0.5% already leads to distortions of the reconstructed temperature profile ($\Delta_T = 2$ K), whereas an error of 3% leads to a significant distortion of the temperature profile (the maximum error Δ_T is 13 K). It is known from the literature that the error in measuring the outgoing radiation does not exceed 1%. Results of our modeling demonstrate that if we take into account all physical uncertainties of the problem (terms of Eq. (1) that are outside the integral), we will obtain the satisfactory accuracy of the reconstructed temperature profile for the above-indicated measurement error.

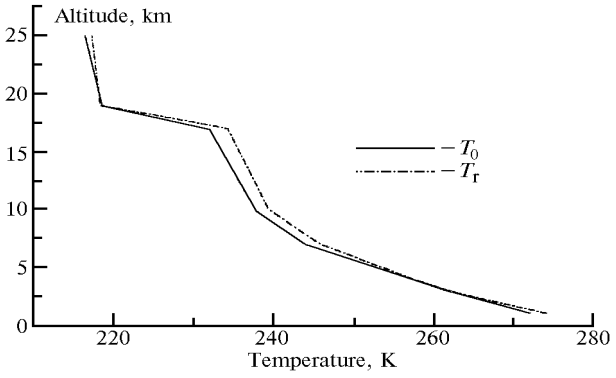

FIG. 2. Reconstructed profile of the temperature T_r in comparison with the model profile of the temperature T_0 (for the midlatitudes in summer) for a noise level of 0.5%.

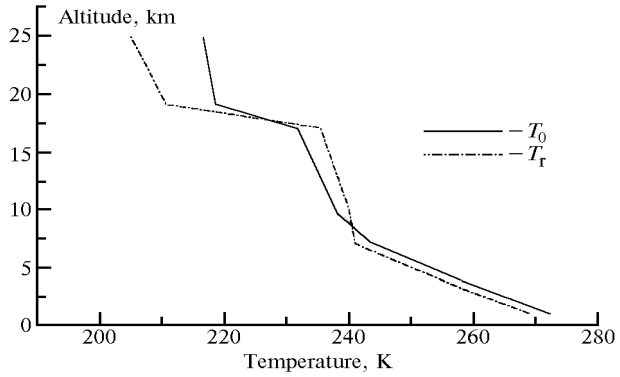

FIG. 3. Reconstructed profile of the temperature T_r in comparison with the model profile of the temperature T_0 (for the mid-latitudes in summer) for a noise level of 3%.

The errors in reconstructing the temperature profiles caused by the errors of spectroscopic measurements and determination of the UST were also examined in Ref. 7. Results of solving the problem by the optimal parametrization and statistical regularization method were presented there.

The vertical profiles of the temperature reconstructed from real measurements in the Arctic are illustrated by Fig. 4. The emission of the underlying surface was modeled and eliminated from the model data. It can be seen from the figure that the reconstructed values of the temperature, at least, do not contradict the common sense and agree with model description of the thermal state of the atmosphere. To be more specific, these data should be compared with corresponding results of radiological sensing of the temperature.

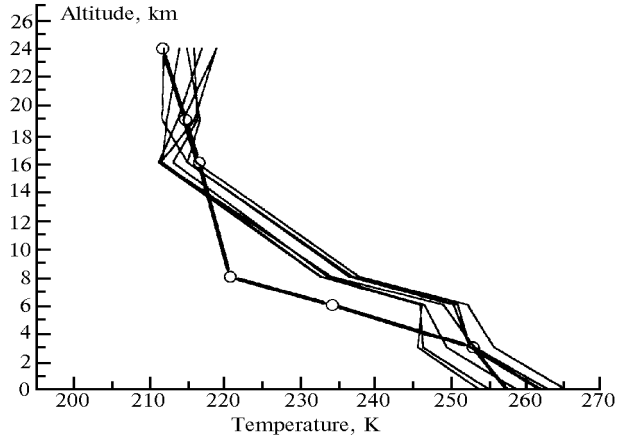

FIG. 4. Reconstructed temperature profiles for several lines in comparison with the model temperature profile (for subarctic summer) denoted by the solid curve with circles).

CONCLUSION

Investigations of the potentialities of the HIRS/2 radiometer for retrieval of gaseous composition and temperature of the atmosphere performed in the present paper have demonstrated that the temperature profiles and the total content of H_2O, O_3, and N_2O can be reconstructed from measurements with this radiometer at night for cloudless atmosphere. The total content of CO and CH_4 cannot be retrieved from measurements with HIRS/2 with satisfactory accuracy.

To develop engineering procedures for retrieval of gaseous composition and temperature in cloudless atmosphere, the following problems should be solved:

1) the underlying surface temperature and its albedo should be determined;

2) the HIRS/2 data measured in the cloudy atmosphere should be rejected.

The problem of determining the temperature and emissivity of the underlying surface is at least no simpler than the problem of determining the atmospheric parameters. Its solution calls for additional measurements with the AVHRR and MSU apparatuses placed onboard the NOAA satellites at the same platform with the HIRS/2 and SSU instruments.

Rejection of measurements in the cloudy atmosphere can be done only on the basis of special procedures with the use of additional physical information, data on the synoptic state of the atmosphere lidar data, etc.

To develop the procedures for determining the atmospheric parameters in the cloudy atmosphere and in particular, under conditions of continuous cloudiness, further investigations and modeling should be carried out.

Measurements with the HIRS/2 radiometer can be used to retrieve the vertical profile of the temperature at altitudes up to 25–27 km. To increase the maximum altitude of temperature sensing up to 50 km, measurements with the SSU stratospheric apparatus can be used.

A solution of the inverse problems on the determination of gaseous composition and temperature of the atmosphere above Tomsk by the methods based on the use of *a priori* information about the examined parameters calls for:

– construction of regional statistical models of vertical distribution of the temperature and water vapor for clear days from the data of aerological observations at the station Novosibirsk nearest to Tomsk;

– to evaluate a cross correlation of the total ozone and water vapor content with the temperature of individual atmospheric altitude levels from the data of total ozone content observations in Tomsk and the data of high-altitude sensing of the temperature and water vapor content at the station Novosibirsk;

– to investigate a cross correlation of the total ozone and water vapor content and the atmospheric temperature at different altitude levels with the radiative temperatures of the HIRS channels.

REFERENCES

1. J. Vazquez, A. Van Tran, et al., NOAA/NASA AVHRR Oceans Pathfinder. Sea Surface Temperature Data Set. User's Guide. Version 1.3. August 29. 1996 (an Internet site).
2. W.G. Planet, ed., Data Extraction and Calibration of TIROS–N/NOAA Radiometers, NOAA Technical Memorandum NESS 107–Rev. 1, Washington, D.C., 1979 (Revised in 1988).
3. L.E. Williamson, Calibration Technology for Meteorology Satellites, Atmospheric Laboratory, U.S. Army Electronics Command, White Sands Missile Range, N.M. (1977).
4. A.C. Neuendorffer, J. Geophys. Res. **101**, No. D13, 18.807–18.828 (1996).
5. A.J. Krueger and R.A. Mizner, J. Geophys. Res. **81**, 4477 (1976).
6. K.M. Firsov, M.Yu. Kataev, V.S. Komarov, and T.Yu. Chesnokova, in: *Abstracts of Reports at the Fifth International Symposium on Atmospheric and Oceanic Optics*, Tomsk (1998).
7. M.Yu. Kataev and A.A. Mitzel', in: *Abstracts of Reports of the Fifth International Symposium on Atmospheric and Oceanic Optics,* Tomsk (1998).
8. M.S. Malkevich, *Optical Investigations of the Atmosphere from Satellites* (Nauka, Moscow, 1973).
9. V.M. Sutovskoi and A.B. Uspenskii, Issled. Zemli iz Kosmosa, No. 4, 75–78 (1985).
10. E.P. McClain, W.G. Pichel, and C.C. Walton, J. Geophys. Res. **90**, No. C6, 11587–11601 (1985).
11. J. Suskind and D. Reuter, J. Geophys. Res., **90**, No. C6, 11602–11608 (1985).
12. W.J. Emery, Y. Yanyue, and G.A. Wick, J. Geophys. Res. **99**, No. C3, 5219–5236 (1994).
13. A.B. Uspenskii, Meteorol. Gidrol., No. 10, 19–27 (1992).
14. F. Becker and Z.L. Li, Remote Sensing of Environm. **32**, 315–318 (1990).
15. K.Ya. Kondrat'ev and Yu.M. Timofeev, *Thermal Sensing of the Atmosphere from Satellites* (Gidrometeoizdat, Leningrad, 1970), 410 pp.
16. A.N. Tikhonov and V.Ya. Arsenin, *Methods for Solving Ill-Posed Problems* (Nauka, Moscow, 1979) 264 pp.